



Coastal amplification of supply and transport (CAST): a new hypothesis about the persistence of *Calanus finmarchicus* in the Gulf of Maine

Rubao Ji^{1*}, Zhixuan Feng¹, Benjamin T. Jones¹, Cameron Thompson², Changsheng Chen³, Nicholas R. Record⁴, and Jeffrey A. Runge²

¹Department of Biology, Woods Hole Oceanographic Institution, Woods Hole, MA 02543, USA

²School of Marine Sciences, University of Maine and Gulf of Maine Research Institute, Portland, ME, USA

³School for Marine Science and Technology, University of Massachusetts Dartmouth, Dartmouth, MA, USA

⁴Bigelow Laboratory for Ocean Sciences, 60 Bigelow Dr, East Boothbay, ME 04544, USA

*Corresponding author: tel: 1-508-289-2986; fax: 1-508-457-2134; e-mail: rji@who.edu.

Ji, R., Feng, Z., Jones, B. T., Thompson, C., Chen, C., Record, N. R., and Runge, J. A. Coastal amplification of supply and transport (CAST): a new hypothesis about the persistence of *Calanus finmarchicus* in the Gulf of Maine. – ICES Journal of Marine Science, doi:10.1093/icesjms/fsw253.

Received 15 August 2016; revised 21 December 2016; accepted 21 December 2016.

The lipid-rich calanoid copepod, *Calanus finmarchicus*, plays a critical role in the pelagic food web of the western North Atlantic and particularly in the Gulf of Maine ecosystem. Deep basins along the continental shelf harbour high abundance of diapausing *C. finmarchicus* during the summer and fall. In Wilkinson Basin in the western Gulf of Maine, *C. finmarchicus* has persisted in large concentrations despite recent significant warming that could potentially threaten the existence of the population in this region. Identifying the major source of diapausing individuals is critical to the understanding of mechanisms that allow population persistence. In this study, Lagrangian tracking experiments using an individual-based copepod life cycle model and simulation of environmental conditions during an exceptionally warm year (2012) suggest that coastal waters are the major upstream source for individuals entering dormancy in Wilkinson Basin over summertime, although pathways and distribution patterns vary with the release timing of particles. Both model results and observation data support the Coastal Amplification of Supply and Transport (CAST) hypothesis as an explanation for the persistence of *C. finmarchicus* population in the western Gulf of Maine. The mechanism involves the coastal amplification of supply (spring reproduction/summer growth in the food-rich coastal region) and transport to the receiving Wilkinson Basin that is capable of harbouring the diapausing stock.

Keywords: *Calanus finmarchicus*, Gulf of Maine, individual based model, life history, population persistence.

Introduction

Warming is a main threat to the existence of many marine organisms that have adapted to certain thermal habitats. For the planktonic copepod, *Calanus finmarchicus*, the Gulf of Maine (GoM) represents the southern edge of its subarctic range (Melle *et al.*, 2014), and thus a relatively small increase of water temperature might have serious consequences for the ability of the species to sustain abundance in the region (Beaugrand, 2012). The shelf waters along the Northeast U.S. coast including the GoM are

expected to see more severe warming than the rest of the North Atlantic (Bopp *et al.*, 2013; Saba *et al.*, 2016). Niche-based statistical models suggest a northward shift of the *C. finmarchicus* biogeographic boundary in a warming climate, and indicate that the population will cease to exist in the GoM over the next several decades (Helaouët and Beaugrand, 2009; Reygondeau and Beaugrand, 2011; Villarino *et al.*, 2015). If these predictions are realized, the structure and function of the GoM ecosystem may be severely impacted, leading to significant disruption of

ecosystem services such as marine biodiversity and fisheries in the region (Johnson *et al.*, 2011).

Over the past decade, sea surface temperature (SST) in the GoM has warmed at a rate ($0.2\text{ }^{\circ}\text{C year}^{-1}$; Mills *et al.*, 2013) that is more than 10 times greater than the 100-year mean rate (Shearman and Lentz, 2010). In 2012, a record warm year, the maximum SST observed in a Wilkinson Basin (WB) station reached $22\text{ }^{\circ}\text{C}$ in late August (Runge *et al.*, 2015). SST in summer was as much as $5\text{ }^{\circ}\text{C}$ higher than the long-term average (Chen *et al.*, 2015). The annual mean SST has exceeded $10\text{ }^{\circ}\text{C}$, a biogeographic indicator for the North Atlantic (Beaugrand *et al.*, 2008), in the western GoM since 2006 and in the eastern GoM since 2012, based on National Oceanographic Data Center Advanced Very High Resolution Radiometer (AVHRR) data. The observed response of *C. finmarchicus* to the 2012 warming has suggested that the population did not show a significant decline in stock size, nor any sign of early lipid depletion in the WB overwintering stock as predicted (Maps *et al.*, 2012; Runge *et al.*, 2015).

Based on these findings, Runge *et al.* (2015) hypothesized that the primary source of late-stage *C. finmarchicus* to WB involves the Maine Coastal Current (MCC) that flows along the coast, centred on the 100-m isobaths, between the Bay of Fundy (BoF) and Cape Cod (Figure 1). *Calanus* copepods originating from the upstream BoF region develop through one or more generations into late copepodid stages as they drift southwestward along the MCC. Supplied by nutrient-rich waters from the eastern GoM, the MCC supports high primary production (Li and He, 2014; Tian *et al.*, 2014), sustaining *C. finmarchicus* growth and reproduction throughout the summer months. Moreover, the temperature in the MCC is cooler and remains in the optimal range for growth during summer, in contrast to the stratified surface waters of the central GoM, which already reach temperatures ($>19\text{ }^{\circ}\text{C}$) considered to be physiologically adverse for *C. finmarchicus* (Preziosi and Runge, 2014). This whole process, termed as the ‘‘Coastal Amplification of Supply and Transport (CAST)’’ hypothesis here, is suggested to contribute significantly to the persistence of *C. finmarchicus* population in the GoM.

The purpose of this study is to test the CAST hypothesis using both model and observational results. Specifically, the transport pathway of the population reaching WB is examined using an individual-based model (IBM) with Lagrangian tracking and copepod life stage development capabilities. The time and spatial scales of transport and the connection to potential supply sites are assessed by comparing the model results with the observed demographic data. Based on these analyses, we discuss the evidence and mechanisms for the coastal amplification process.

Material and methods

Physical model

The third generation Gulf of Maine-Finite Volume Community Ocean Model (GoM-FVCOM; Chen *et al.*, 2007) was used to represent hydrographic and hydrodynamic conditions in the study region and to provide necessary model forcing for simulating copepod Lagrangian tracking and life stage development. GoM-FVCOM is a circulation model of the northeast coastal system with horizontal resolutions ranging from 0.3 to 10 km (Cowles *et al.*, 2008; Chen *et al.*, 2011; Xue *et al.*, 2014). This regional model is nested within the FVCOM-Global model with common mesh zones that ensure mass and water property conservation (Chen *et al.*, 2011). GoM-FVCOM is the core ocean model in the

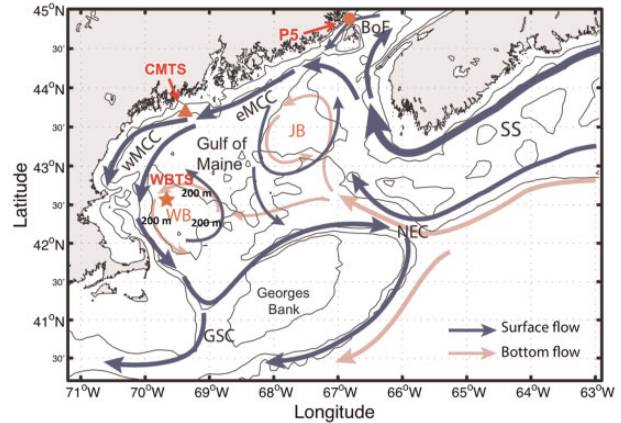


Figure 1. The Gulf of Maine region with schematic mean circulation pattern and locations of three plankton survey stations: WBTS (Wilkinson Basin Time Series; star marker), CMTS (Coastal Maine Time Series; triangle marker) and P5 (Prince 5 from Canada’s AZMP program; circle marker). BoF, Bay of Fundy; NS, Nova Scotia; SS, Scotian Shelf; NEC, Northeast Channel; GB, Georges Bank; GSC, Great South Channel; WB, Wilkinson Basin. Isobaths represent 50, 100 and 200 m. The 200-m isobaths surrounding WB are labeled.

Northeast Coastal Ocean Forecast System (NECOFS), which became operational in 2007 (<http://fvcom.smast.umassd.edu>). In its third generation, GoM-FVCOM has been run for the period between 1978 and 2013, and the hourly model field is available on the NECOFS server. The model assimilates satellite-derived SST, and CTD profile data from buoys and field surveys (Xue *et al.*, 2014), and thus accurately reproducing the temperature fields needed for the purpose of this study. The model has accurately simulated the short- (hourly to daily) and long-term (seasonal to interannual) water stratification (Xue *et al.*, 2014; Li *et al.*, 2015), and currents (Chen *et al.*, 2011; Sun *et al.*, 2016). Its Lagrangian-tracking capabilities have been demonstrated through comparisons of GoM-FVCOM-derived virtual drifter trajectories with observed trajectories of 681 surface drifters (Sun, 2014).

Individual-based model (IBM)

An IBM was utilized to conduct copepod Lagrangian tracking and life stage development experiments (Ji *et al.*, 2012; Boucher *et al.*, 2013; Liu *et al.*, 2015). The model simulations were conducted in the so-called ‘‘offline’’ mode, i.e. the GoM-FVCOM simulations were conducted prior to the IBM runs to provide flow fields for Lagrangian tracking and temperature for copepod life stage development (Figure 2). Both flow and temperature fields are stored to allow multiple numerical experiments later, precluding the need to re-run the physical model. This procedure provides higher computing efficiency than the ‘‘online’’ mode, in which the physical model and the IBM are run together. The numerical experiments were conducted specifically for the 2012 case study.

The Lagrangian tracking model solves the advection equation using a fourth order Runge-Kutta (RK-4) method. The stage-based life cycle model resolves copepod life stage progression through all 13 developmental stages (Figure 2c). The temperature- and food-dependent development time (or rate) follows Bělehrádek (Bělehrádek, 1935; McLaren, 1963) and Ivlev (1955)

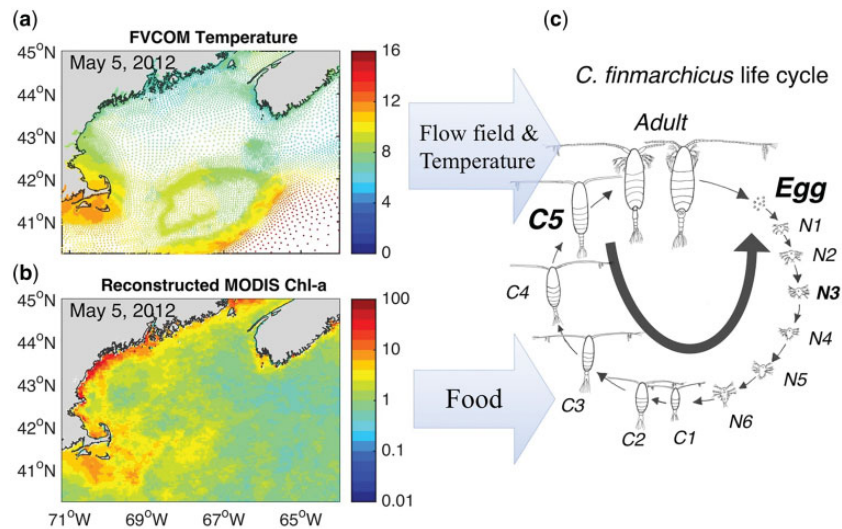


Figure 2. The offline model coupling between FVCOM and IBM (see text for explanation of abbreviations). The FVCOM-simulated hourly flow fields are interpolated in the IBM to obtain current velocities for Lagrangian tracking of *C. finmarchicus* individuals. FVCOM-simulated temperature and reconstructed MODIS chlorophyll-*a* concentration are also interpolated for use in calculating *C. finmarchicus* life stage development. (a) A snapshot of FVCOM-simulated ocean surface temperature ($^{\circ}\text{C}$) at 00:00 GMT 5 May 2012. The temperatures are plotted at corresponding FVCOM grid nodal points. (b) A snapshot of reconstructed chlorophyll-*a* concentration (mg m^{-3}) in 5 May 2012. (c) Thirteen life stages of *C. finmarchicus*. N3 is the first feeding stage when food is required for life stage development, and C5 is the diapausing stage for *C. finmarchicus*. In the numerical experiments, all *C. finmarchicus* individuals are backward tracked and life stages are reversed from older to younger stages.

functions (Figure 3). The Bělehrádek function quantifies the temperature-dependent development time in each life stage, which exponentially decreases with higher temperature under the food-saturated conditions (Figure 3a). The Ivlev function is used as a dimensionless coefficient to protract the development time under the food-limited conditions (Figure 3b). The model coefficients are fitted to the laboratory measurements of *C. finmarchicus* growth and development rates (Campbell *et al.*, 2001). Model formulations and details can be found in Ji *et al.* (2012). For this study, in order to assess the possible source region of individuals with known ending locations, the tracking simulations were conducted backward in time: particles were tracked backward by reversing the flow field. This approach is similar to the ones used by Batchelder (2006) and Pepin *et al.* (2013). In this study, the stage development of *C. finmarchicus* was also reversed so the total duration of backward tracking for each individual can be determined. The caveats of backward-in-time tracking are discussed later in this article.

For simulating copepod life stage development, temperature is temporally and spatially interpolated using GoM-FVCOM forcing (Figure 2a). NASA's Moderate Resolution Imaging Spectroradiometer (MODIS) chlorophyll-*a* concentrations (mg m^{-3}) are used to retrieve food conditions (Figure 2b). To remove data gaps resulting from cloud coverage, the daily gridded MODIS chlorophyll-*a* concentrations are processed and reconstructed using the Data Interpolation Empirical Orthogonal Function (DINEOF) method (Li and He, 2014). Then, the reconstructed chlorophyll-*a* data are mapped onto the unstructured mesh of GoM-FVCOM so that the inherent interpolation schemes in Lagrangian tracking model can be used to calculate copepod individuals' instantaneous chlorophyll-*a* (food) concentrations.

Zooplankton surveys

Semimonthly to monthly observations of zooplankton diversity and abundance, including stage composition of *C. finmarchicus*, are available at three fixed time series stations (Figure 1): Prince-5 (P5: $44^{\circ}51.0' \text{ N}$; $66^{\circ}58.2' \text{ W}$; depth: 95 m), located in the BoF, the Coastal Maine Time Series (CMTS: $43^{\circ}44.8' \text{ N}$, $69^{\circ}30.1' \text{ W}$; depth: 105 m), located on the western edge of the Maine Coastal Current, and the Wilkinson Basin Time Series (WBTS: $42^{\circ}51.7' \text{ N}$, $69^{\circ}51.8' \text{ W}$; depth: 225 m), located in the northwestern corner of WB. Following protocols established by the Canadian Atlantic Zonal Monitoring Program (AZMP), *C. finmarchicus* abundance and stage structure is estimated from zooplankton samples collected with 0.75 m diameter, 200- μm mesh ring nets towed from near bottom to the surface (Mitchell *et al.*, 2002; Runge *et al.*, 2015). The Station P5 *C. finmarchicus* abundance and stage distribution data are obtained from Fisheries and Ocean Canada (<http://www.meds-sdmm.dfo-mpo.gc.ca/>) through the AZMP. The CMTS and WBTS data are available from the Biological & Chemical Oceanography Data Management Office (BCO-DMO) database (<http://www.bco-dmo.org/>). Additionally, Laser Optical Plankton Counter (LOPC) profiles are available at the WBTS station for the cruises from 24 May through 7 August 2012. Upcast data, which was filtered to include particles with properties associated with large copepods, was used to identify layers of late-stage *C. finmarchicus*. Particles with a computed equivalent spherical diameter (d) in the range $1000 \mu\text{m} < d < 2500 \mu\text{m}$, and with attenuation proportion (α) in the range $0.25 < \alpha < 0.6$, were included. The range of d was based on the equivalent spherical size of late-stage *C. finmarchicus*, and the range of α was based on the *in situ* laser optical properties of a population of diapausing copepods observed in WB (Runge *et al.*, 2012). The attenuation proportion and particle size range are comparable to prior studies

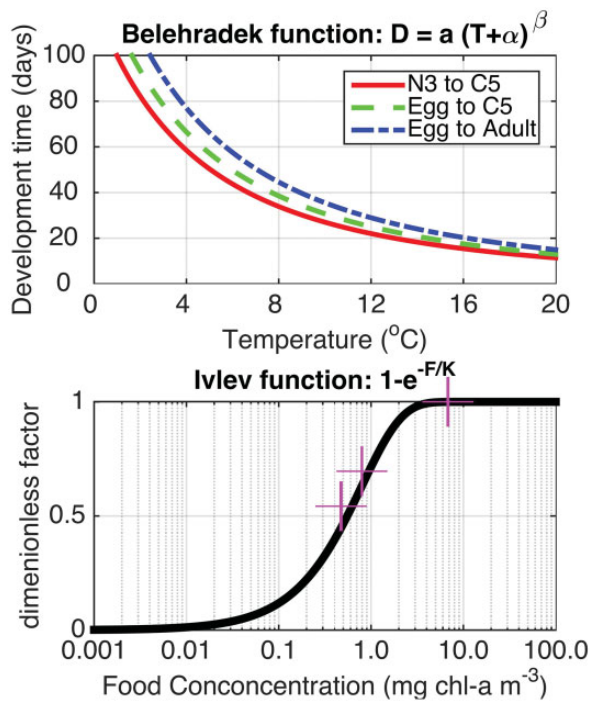


Figure 3. Model formulation for *C. finmarchicus* development as a function of temperature (upper panel, showing development time at non-limiting food conditions) and food (lower panel, showing factor by which maximum development time is divided at respective limiting food concentrations).

that estimated *C. finmarchicus* from LOPC casts (Checkley et al., 2008; Gaardsted et al., 2010).

Numerical experiments

The main objective of the present study is to identify potential upstream source regions that supply diapausing C5 *C. finmarchicus* populations to WB during the summer and fall seasons in the abnormal warm year of 2012 (i.e. test CAST hypothesis). Source tracking of egg spawning sites for two consecutive generations can be achieved by combining backward-in-time Lagrangian tracking with reversed copepod life stage development. A series of ensemble runs were conducted in the months of July and September 2012 to backward track two *C. finmarchicus* generations from WB. The July runs represent *C. finmarchicus* that initiate diapause in early to mid-summer, while the September runs represent late summer to early fall diapausing populations.

Two consecutive simulations, each representing one generation, were conducted to backward track diapause-competent *C. finmarchicus* individuals in WB. At the beginning of each Julian day in July and September, all 91052 Generation-2 (G2) individuals of diapause-competent C5 (i.e. midway between C5 and adult stages) were uniformly released every 200 m inside WB (defined as the area deeper than 220 m). Two types of vertical behaviour are simulated: one with all individuals assumed to be buoyant and remain at the ocean surface (i.e. 0 m), and the other with individuals of late copepodid stages (C4 and C5) capable of diel vertical migration (DVM) between surface and 40 m depth. The DVM allows stages C4 and C5 individuals to migrate in the water column between 0 (optimal night-time depth) and 40 m

(optimal daytime depth), and follows the formulation of Zakardjian et al. (1999). All individuals are backward advected by GoM-FVCOM currents every 10 min (i.e. physical time step). The individuals' ages and corresponding life stages are backward calculated hourly (i.e. biological time step) using instantaneous temperature- and food-dependent development rates and a forward Euler scheme. During the post-processing, the date and geographic location that an individual copepod reverses back to the egg stage are recorded and regarded as a putative egg spawning region for the corresponding adult female of the prior generation (i.e. G1). The egg locations and dates of G2 individuals are used to initialize the second run to backward track G1 individuals from adults to their egg spawning regions, assuming that G1 adults lay eggs immediately after they reach the adult stage. The final geographic locations of G1 and G2 egg individuals are mapped onto a 0.05-degree mesh to generate frequency distributions of two consecutive *C. finmarchicus* generations that may supply diapause-competent *C. finmarchicus* individuals to the WB during summer and fall seasons.

Results

Passive physical tracking

First, all *C. finmarchicus* individuals were initialized from the WB as surface particles without biological dynamics. The spatial distributions of the backward-tracked individuals after 30- and 60-d periods demonstrate that the coastal area is the main upstream source region, but the distributional patterns are different between July and September (Figure 4). For those individuals released in July, the centres of the distribution after 30-d backward tracking are located northeast of the WB, extending along the 50- to 100-m isobaths until the US/Canada border (Figure 4a). After 60-d tracking, the source area of individuals becomes widespread along the GoM shelves, and some individuals can be traced back to BoF and further to the southern Scotian Shelf (Figure 4b). In comparison, the source area of 30-d backward tracked September individuals is more concentrated and located to the west, northwest, and north of the WB, and distributed along the coast from the Massachusetts Bay to southern Maine coast (Figure 4c). With one more month of additional tracking, the distributions of September-released individuals can be traced further northeastward, but are not as extensive as the July release (Figure 4d).

Tracking with life history characteristics

Temperature and food-dependent backward tracking in time yields predictions of egg spawning sites that directly supply diapause-competent individuals to WB. In the month of July, egg spawning sites are mainly located to the north and northeast of WB along the Maine coast (Figure 5a), with an average development time of ~20 d from egg to diapausing C5. The G1 origin (egg stage, two generations back) is much more dispersed on the coastal Maine shelf (Figure 5b) than the G2 origin (egg stage, current generation). The G1 has an average generation time of ~40 d (i.e. in the month of May, ~60 d back from July releases). The centres of egg spawning regions of the current generation in DVM runs are slightly further upstream the MCC than in the surface-keeping runs (Figure 5c).

The egg spawning regions of *C. finmarchicus* individuals that are released from WB in September mainly distribute to the west, northwest, and north of WB (Figure 5c). The average time

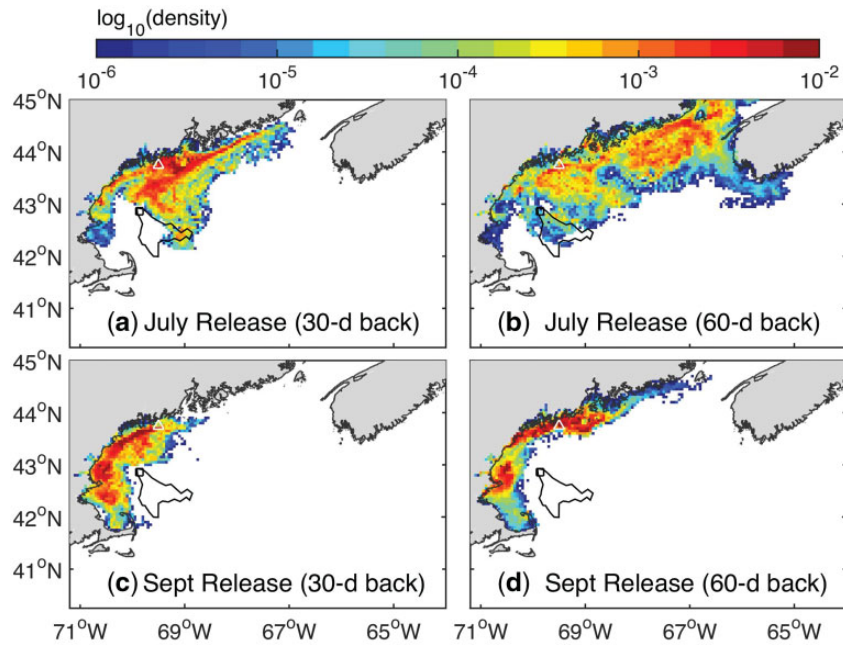


Figure 4. Passive, backward tracking of surface layer particles (no biology) in July after 30 and 60 d (Panels a and b) and in September after 30 and 60 d (Panels c and d). All particles are released within the black line polygon (220 m isobath of the Wilkinson Basin). The CMTS and WBTS stations are indicated by triangle and square symbols.

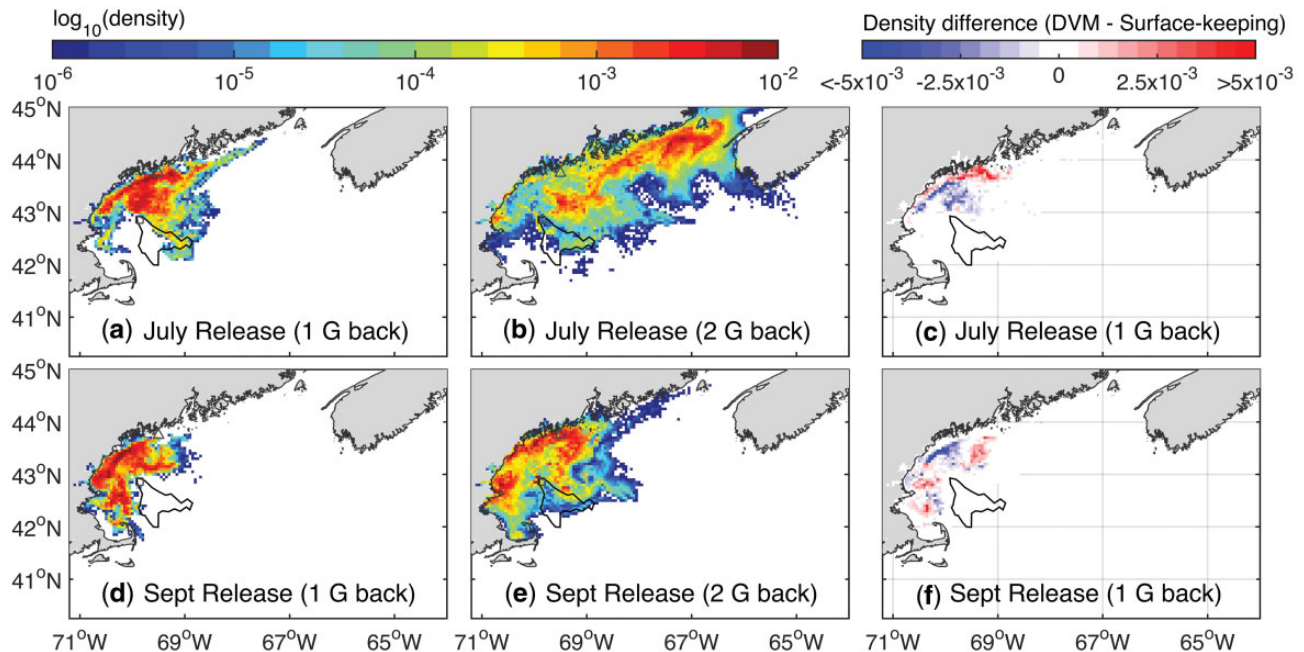


Figure 5. Potential *C. finmarchicus* egg spawning sites (source regions) that may seed WB C5 diapausing populations in (a and b) July and (d–e) September 2012 based on surface-keeping runs, and the distribution differences of source regions between diel vertical migration (DVM) and surface-keeping runs in (c) July and (f) September. The egg spawning sites are determined by temperature and food-dependent backward-in-time tracking of C5 individuals from the WB to their source regions where individuals stage reverts to the egg stage. “1 G back” indicates one generation back; and “2 G back” indicates two generations back. All particles are released within the black line polygon (220 m isobath of the Wilkinson Basin). The CMTS and WBTS stations are indicated by triangle and square symbols.

required for individuals developing from egg to C5 is also 20 d, similar to the July individuals. The distributions of G1 origin (egg stage, two generations back) is slightly more dispersed than G2 eggs, although overall patterns seem similar (Figure 5d).

The average generation time of the G1 individuals is ~ 30 d (i.e. mid-July to mid-August, ~ 50 d back from September releases). The DVM simulations result in similar distribution patterns of egg spawning regions to those of surface-keeping simulations,

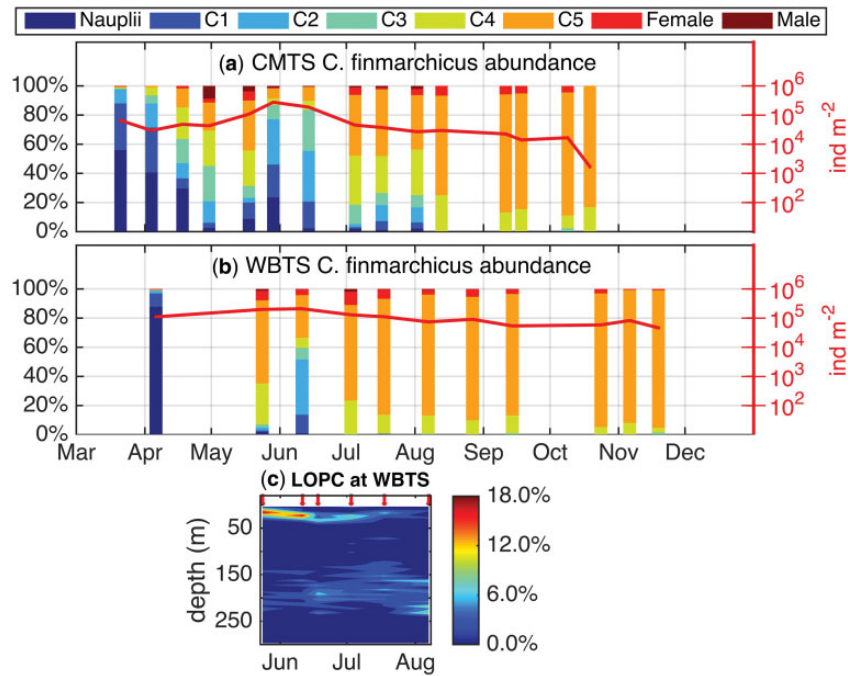


Figure 6. Total abundances and stage composition (relative abundances) of *C. finmarchicus* from March to November 2012 at (a) CMTS and (b) WBTS, and (c) profiles of particles characteristic of late-stage *C. finmarchicus* measured by the LOPC, shown as the proportion of particles in each depth bin. In first two panels, the total abundances (ind m^{-2}) of *C. finmarchicus* are shown by curves in the logarithmic scale. In the panel (6c), the arrows indicate sampling dates.

with minor differences in the vicinity of distribution centres (Figure 5f).

Observations

Observations of *C. finmarchicus* abundance in the MCC at CMTS in 2012 show large numbers of nauplius and copepodid stages in late spring and summer (Figure 6a). Total abundance of copepodid stages C1–C5 was $\sim 2.5 \times 10^4 \text{ ind. m}^{-2}$ in late April and early July, peaking in the interim to as high as $2 \times 10^5 \text{ ind. m}^{-2}$ in late May. Nauplii and stage C1–C2 were present in July/early August at densities $> 1 \times 10^3 \text{ ind. m}^{-2}$, and stages C4–C5 were present throughout the summer up until mid-September, and densities $> 1 \times 10^4 \text{ ind. m}^{-2}$. Thus, there was ample abundance of *C. finmarchicus* life stages in the MCC during the period indicated by the backward tracking model for supply to WB.

In WB, large abundances of early life stages (nauplius and stages C1–C2), up to $1 \times 10^5 \text{ ind. m}^{-2}$, were present through mid-June, after which the stage composition was dominated by stages C4–C5 at densities ranging between 2.5 and $8.5 \times 10^4 \text{ ind. m}^{-2}$ through mid-November (Figure 6b). The LOPC profiles show two distinct layers of particles characteristic of late-stage *C. finmarchicus*: one between 30 m and the surface, and one deeper than 150 m, of varying depths (Figure 6c). The shallow layer diminishes through the time series, with only a tiny proportion of particles in the surface waters by August. The proportion of particles (with properties associated with large copepods) in the deep layer has a corresponding increase, with a very small proportion of particles at depth in May, and most of the particles at depth by August.

Discussion

The results of this Lagrangian experiment are consistent with the hypothesis that a major source of supply of *C. finmarchicus* to WB derives from late spring and summer production in the MCC. Stages C4–C5 were abundant at the CMTS station in the MCC throughout the summer (Figure 6a), and the particle tracking results (Figure 4a and c) show that cross-shelf transport of these stages from the coastal shelf to WB is possible. Observations at the CMTS (Figure 6a) show the presence of *C. finmarchicus* females and early life stages at the time of origin indicated by the backward tracking results to egg spawning sites (Figure 5).

The model results (Figures 4 and 5) also suggested that the *C. finmarchicus* population can go through multiple generations along the food-rich Maine coastal region. This could potentially allow the population to grow due to high reproduction and development rates while being transported from the upstream BoF region to WB. Without fully resolved population dynamics from either observations or modelling, it is difficult to test this hypothesis directly. However, evidence from three sites along the population transport pathway, suggesting that abundance of both C5s and adults increase from the upstream site P5 to CMTS and eventually to WBTS in both spring (Figure 7a) and summer (Figure 7b) conditions, is consistent with the CAST concept. As the water temperature in the MCC is higher during the summertime than the springtime, it is likely that the population can go through more generations in summertime, which can further amplify the upstream source population. Since the source of water for the MCC, from the BoF and eastern GoM, ensures colder temperatures within the optimal range for *C. finmarchicus*, even in summer, the CAST hypothesis offers a mitigating mechanism to offset the potential detrimental effects of warming in the deeper, central GoM.

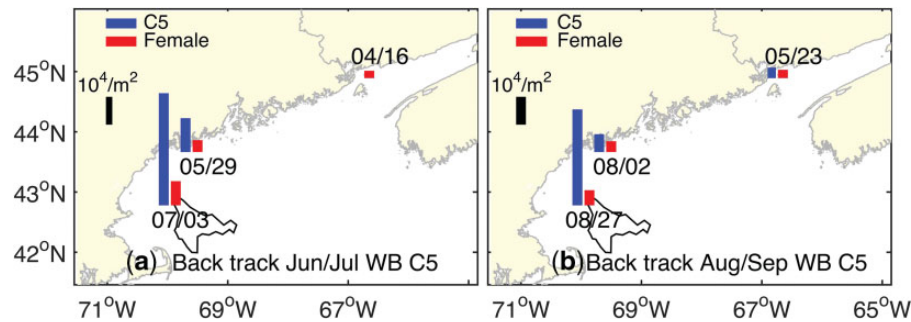


Figure 7. Observed abundance of C5 and adult female *Calanus finmarchicus* at the WBTS, CMTS and P5 during the dates that approximately match the advective timescale of water mass. (a) Spring scenario: the upstream P5 station sampling time in mid-April and the downstream WB station sampling time in early July; (b) Summer scenario: the upstream P5 station sampling time in late May and the downstream WB station sampling time in late August.

Combining the models and the observational evidence, a conceptual model of CAST dynamics is illustrated here (Figure 8). The BoF is a potential source region that supplies the seed population to the downstream Maine coast and eventually reaching WB. The C5 individuals reach WB during early-mid-summer (Figure 8, left panel) could be the direct offspring of the BoF adults or through one additional generation; whereas the C5 individuals reaching WB in later-summer and fall are more likely to go through one or two more generations (Figure 8, right panel). It is worth noting that this conceptual model needs to be investigated in future studies, ideally through a direct high-resolution observation of population structure along the MCC, such that the along-shelf stage succession from egg to nauplii and further to copepodites can be detected.

The tracking experiment conducted here examines transport of copepods at the ocean surface and with a DVM behavior. The vertical distribution of *C. finmarchicus* copepodid stages in summer in the MCC, which is relatively shallow (centered on 100 m: Churchill *et al.*, 2005) is not well known. Observations of vertical distribution of actively growing stages C4–C5 in the lower St. Lawrence Estuary in July (Plourde *et al.*, 2001) showed stages C1–C3 in the upper 25 m day and night and a possible diel migration to the surface 25 m by stages C4–C5. The presence of actively growing stage C4–C5 in the surface 25 m was also observed by Sameoto and Herman (1990) in Emerald Basin in June and by Durbin *et al.* (1997) in the southern GoM in November. The source tracking results of DVM runs show that distribution patterns of G2 origin (current generation) closely resemble those of surface-keeping runs in both July and September (Figure 5c and f). Further refinement of the transport of *C. finmarchicus* in the MCC awaits more complete data on their day/night vertical distribution patterns.

It is worth pointing out that although the above DVM experiments have not suggested significant sensitivity of source regions to diel migrations, other behaviours not included in the model could still lead to different transport pathways and sources. At a fine spatial scale (e.g. \sim cm to m), spatial gradients of flow velocity and fluid density are known to induce changes in copepods' swimming behavior and local residence time, and may therefore affect large-scale population dispersal and connectivity (Woodson *et al.*, 2005, 2007; McManus & Woodson, 2012; True *et al.*, 2015). In regions like the GoM coast, various physical gradients exist, ranging from strong tidal mixing front across the shelf to density stratification vertically. These physical gradients are generally associated with biological aggregation and

patchiness, including phytoplankton enhancement in frontal zones and thin layers. Although the model in this study cannot resolve this fine-scale details yet, the potential of its impact on dispersion and connectivity must not be ignored and the sensitivity should be tested in future studies.

Local production within WB must also be another source of stage C5 in summer and fall in WB (as also implied by a tracking study of Johnson *et al.*, 2006). Clearly, there was a strong cohort production in WB in late spring (Figure 6b), which certainly contributed substantially to the stock of stage C5 in WB, especially in early summer. However, the temperature at depth where the C5 stages reside in WB is warm relative to the species' normal sub-arctic habitat, and life cycle models including metabolism of lipid stores indicate that stage C5 entering into diapause in late spring/early summer must emerge to molt into females in fall/early winter (Maps *et al.*, 2012). Early emergence from diapause in late fall in the southern GoM has been observed by Durbin *et al.* (1997). Moreover, Runge *et al.* (2015) observed that stage C5 in WB in late September, 2012, had the appearance of newly dormant individuals, replete with large lipid stores. Thus, supply of new individuals from the coastal shelf is seen to make an important contribution to the WB diapausing stock.

The possible source population regions were derived from backward-in-time tracking approach, which has some known caveats. The results could be sensitive to the subgrid-scale dispersal pattern applied in the simulation (Pepin and Helbig, 1997; Pepin *et al.*, 2013). One of the difficulties in the backward-in-time tracking is the irreversibility of the stochastic diffusion processes as pointed out by Pepin and Helbig (1997), although both studies by Batchelder (2006) and Christensen *et al.* (2007) have shown that the backward tracking can give a reasonable estimate of the spatial probability distribution of source regions when the tracking time scale and model's spatial resolution are set carefully. In this study, no subgrid-scale dispersion was included in order to avoid the irreversibility issue, although the model is probably still not able to capture the fine-scale dispersal even with a relatively high-horizontal resolution (\sim 0.5 km nearshore) and short integration time ($<$ 2 months in general). The model results should be used only to assess potential source regions, but not to locate where the reproduction actually occurred.

The conventional method for forecasting species distributions under changing climate scenarios is the bioclimate envelope approach, as implemented in species distribution models, habitat distribution models and habitat suitability models (Box, 1981;

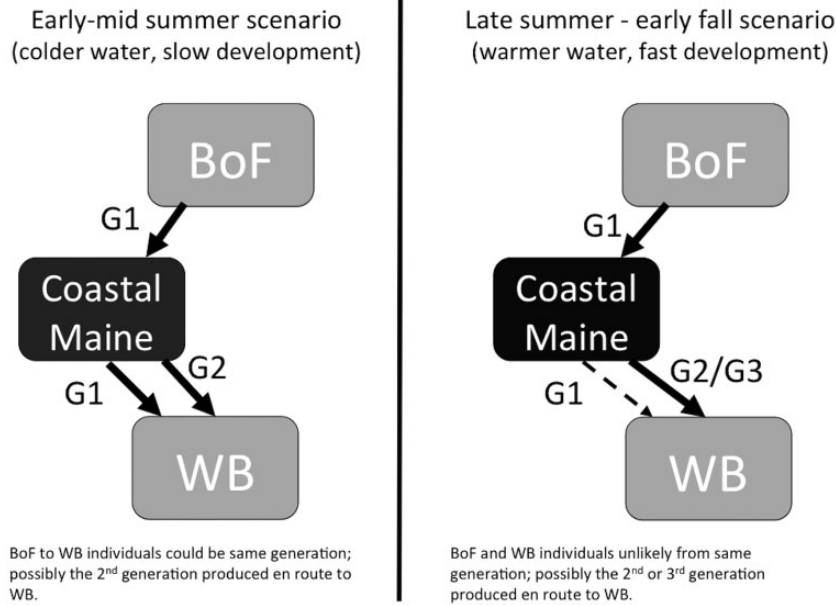


Figure 8. A conceptual model illustrating the connection from BoF to coastal Maine and eventually to WB through MCC. The population goes through one or two generations in the early—mid-summer period (left panel) and two to three generations for the population in the late summer—early fall period (right panel) while being transported along the MCC.

Guisan and Zimmermann, 2000; Elith and Leathwick, 2009; Hirzel *et al.*, 2011). The approach utilizes empirical relationships among a species' distribution and climate variables to make statistical biogeographic projections onto future climate scenarios, and has been widely applied to predict *C. finmarchicus* colonization/distinction in the North Atlantic (Helaouët and Beaugrand, 2009; Reygondeau and Beaugrand, 2011; Villarino *et al.*, 2015). However, one of the basic tenets of the oceanographic perspective is that the environment is Lagrangian. The occurrence of an organism at a location is not necessarily a function of the climate conditions at that location, but rather the conditions along a Lagrangian path that may extend hundreds of km. In the Northwest Atlantic region, the role of advection in controlling coastal *C. finmarchicus* population dynamics is evident (Pepin *et al.*, 2013). It is a combination of the conditions along the advection path and the upstream supply that ultimately determine the presence and abundance of a species. In the ocean, advection can transport the population through productive conduits, creating persistent abundant population centres well outside of a species' expected range. Understanding the interplay between advective supply and local production in complex but important boundary regions on coastal shelves, like the GoM, is essential to predicting range shifts and ecosystem consequences in the changing ocean environment.

Acknowledgements

This work is funded by National Science Foundation (NSF) Division of Ocean Sciences (OCE-1459133, 1459087, 1459092, and 1459096). The NECOF hindcast product is built using the regional-global nested FVCOM system. The global-FVCOM effort was supported by the NSF project under grant number OCE109341. We thank the following colleagues for valuable discussions: Peter Wiebe, Cabell Davis, Frédéric Maps, and Catherine Johnson. Some results were presented at ICES/PICES

6th Zooplankton Production Symposium in Bergen, Norway. We thank Yizhen Li for sharing reconstructed NASA MODIS ocean colour data. We gratefully acknowledge two anonymous reviewers for constructive comments.

References

- Batchelder, H. P. 2006. Forward-in-time-/backward-in-time-trajectory (FITT/BIIT) modeling of particles and organisms in the coastal ocean. *Journal of Atmospheric and Oceanic Technology*, 23: 727.
- Beaugrand, G. 2012. Unanticipated biological changes and global warming. *Marine Ecology Progress Series*, 445: 293–301.
- Beaugrand, G., Edwards, M., Brander, K., Luczak, C., and Ibanez, F. 2008. Causes and projections of abrupt climate-driven ecosystem shifts in the North Atlantic. *Ecology Letters*, 11: 1157–1168.
- Bělehrádek, J. 1935. *Temperature and Living Matter*. Protoplasma-Monogr, 8. Borntraeger, Berlin. 1–277 pp.
- Bopp, L., Resplandy, L., Orr, J. C., Doney, S. C., Dunne, J. P., Gehlen, M., Halloran, P. *et al.* 2013. Multiple stressors of ocean ecosystems in the 21st century: projections with CMIP5 models. *Biogeosciences*, 10: 6225–6245.
- Boucher, J. M., Chen, C., Sun, Y., and Beardsley, R. C. 2013. Effects of interannual environmental variability on the transport-retention dynamics in haddock *Melanogrammus aeglefinus* larvae on Georges Bank. *Marine Ecology Progress Series*, 487: 201–215.
- Box, E. O. 1981. Predicting physiognomic vegetation types with climate variables. *Vegetatio*, 45: 127–139.
- Campbell, R. G., Wagner, M. M., Teegarden, G. J., Boudreau, C. A., and Durbin, E. G. 2001. Growth and development rates of the copepod *Calanus finmarchicus* reared in the laboratory. *Marine Ecology Progress Series*, 221: 161–183.
- Checkley, D. M., Davis, R. E., Herman, A. W., Jackson, G. A., Beanlands, B., and Regier, L. A. 2008. Assessing plankton and other particles in situ with the SOLOPC. *Limnology and Oceanography*, 53: 2123–2136.
- Chen, C., Huang, H., Beardsley, R. C., Liu, H., Xu, Q., and Cowles, G. 2007. A finite volume numerical approach for coastal ocean

- circulation studies: comparisons with finite difference models. *Journal of Geophysical Research: Oceans*, 112: 1–34.
- Chen, C., Huang, H., Beardsley, R. C., Xu, Q., Limeburner, R., Cowles, G. W., Sun, Y. *et al.* 2011. Tidal dynamics in the Gulf of Maine and New England Shelf: an application of FVCOM. *Journal of Geophysical Research: Oceans*, 116: 1–14.
- Chen, K., Gawarkiewicz, G., Kwon, Y. O., and Zhang, W. 2015. The role of atmospheric forcing versus ocean advection during the extreme warming of the Northeast U.S. continental shelf in 2012. *Journal of Geophysical Research: Oceans*, 120: 4324–4339.
- Christensen, A., Daewel, U., Jensen, H., Mosegaard, H., St John, M. A., and Schrum, C. 2007. Hydrodynamic backtracking of fish larvae by individual-based modelling. *Marine Ecology Progress Series*, 347: 221–232.
- Churchill, J. H., Pettigrew, N. R., and Signell, R. P. 2005. Structure and variability of the Western Maine Coastal Current. *Deep-Sea Research II*, 52: 2392–2410.
- Cowles, G. W., Lentz, S. J., Chen, C., Xu, Q., and Beardsley, R. C. 2008. Comparison of observed and model-computed low frequency circulation and hydrography on the New England shelf. *Journal of Geophysical Research: Oceans*, 113: 1–17.
- Durbin, E. G., Runge, J. A., Campbell, R. G., Garrahan, P. R., Casas, M. C., and Plourde, S. 1997. Late fall-early winter recruitment of *Calanus finmarchicus* on Georges Bank. *Marine Ecology Progress Series*, 151: 103–114.
- Elith, J., and Leathwick, J. 2009. Species distribution models: ecological explanation and prediction across space and time. *Annual Review of Ecology, Evolution, System*, 40: 677–697.
- Gaardsted, F., Tande, K. S., and Basedow, S. L. 2010. Measuring copepod abundance in deep-water winter habitats in the NE Norwegian Sea: intercomparison of results from laser optical plankton counter and multinet. *Fisheries Oceanography*, 19: 480–492.
- Guisan, A., and Zimmermann, N. E. 2000. Predictive habitat distribution models in ecology. *Ecological Modelling*, 135: 147–186.
- Helaouët, P., and Beaugrand, G. 2009. Physiology, ecological niches and species distribution. *Ecosystems*, 12: 1235–1245.
- Hirzel, A. A. H., Hausser, J., Chessel, D., and Perrin, N. 2011. Ecological-niche factor analysis: how to compute habitat-suitability maps without absence data? *Ecology*, 83: 2027–2036.
- Ivlev, V. S. 1955. Experimental ecology of nutrition of fishes. *Bulletin of Mathematical Biophysics*, 19: 237–240.
- Ji, R., Ashjian, C. J., Campbell, R. G., Chen, C., Gao, G., Davis, C. S., Cowles, G. W. *et al.* 2012. Life history and biogeography of *Calanus* copepods in the Arctic Ocean: an individual-based modeling study. *Progress in Oceanography*, 96: 40–56.
- Johnson, C., Pringle, J., and Chen, C. 2006. Transport and retention of dormant copepods in the Gulf of Maine. *Deep-Sea Research Part II: Topical Studies in Oceanography*, 53: 2520–2536.
- Johnson, C. L., Runge, J. A., Alexandra Curtis, K., Durbin, E. G., Hare, J. A., Incze, L. S., Link, J. S. *et al.* 2011. Biodiversity and ecosystem function in the Gulf of Maine: pattern and role of zooplankton and pelagic nekton. *PLoS One*, 6: e16491.
- Li, Y., and He, R. 2014. Spatial and temporal variability of SST and ocean color in the Gulf of Maine based on cloud-free SST and chlorophyll reconstructions in 2003–2012. *Remote Sensing of Environment*, 144: 98–108.
- Li, Y., Fratantoni, P. S., Chen, C., Hare, J. A., Sun, Y., Beardsley, R. C., and Ji, R. 2015. Spatio-temporal patterns of stratification on the Northwest Atlantic shelf. *Progress in Oceanography*, 134: 123–137.
- Liu, C., Cowles, G. W., Churchill, J. H., and Stokesbury, K. D. E. 2015. Connectivity of the bay scallop (*Argopecten irradians*) in Buzzards Bay, Massachusetts, U.S.A. *Fisheries Oceanography*, 24: 364–382.
- Maps, F., Runge, J. A., Leising, A., Pershing, A. J., Record, N. R., Plourde, S., and Pierson, J. J. 2012. Modelling the timing and duration of dormancy in populations of *Calanus finmarchicus* from the Northwest Atlantic shelf. *Journal of Plankton Research*, 34: 36–54.
- McLaren, I. A. 1963. Effects of temperature on growth of zooplankton, and the adaptive value of vertical migration. *Journal of Fisheries Research Board of Canada*, 20: 685–727.
- McManus, M. A., and Woodson, C. B. 2012. Plankton distribution and ocean dispersal. *Journal of Experimental Biology*, 215: 1008–1016.
- Melle, W., Runge, J., Head, E., Plourde, S., Castellani, C., Licandro, P., Pierson, J. *et al.* 2014. The North Atlantic Ocean as habitat for *Calanus finmarchicus*: environmental factors and life history traits. *Progress in Oceanography*, 129: 244–284.
- Mills, K. E., Pershing, A., Brown, C., Chen, Y., Chiang, F. S., Holland, D., Lehuta, S. *et al.* 2013. Fisheries management in a changing climate: lessons from the 2012 ocean heat wave in the Northwest Atlantic. *Oceanography*, 26: 191–195.
- Mitchell, M. R., Harrison, G., Pauley, K., Gagné, A., Maillet, G., and Strain, P. 2002. Atlantic zonal monitoring program sampling protocol. Fisheries & Oceans Canada, Maritimes Region, Ocean Sciences Division, Bedford Institute of Oceanography.
- Pepin, P., and Helbig, J. A. 1997. Distribution and drift of Atlantic cod (*Gadus morhua*) eggs and larvae on the northeast Newfoundland Shelf. *Canadian Journal of Fisheries and Aquatic Sciences*, 54: 670–685.
- Pepin, P., Han, G., and Head, E. J. 2013. Modelling the dispersal of *Calanus finmarchicus* on the Newfoundland shelf: implications for the analysis of population dynamics from a high frequency monitoring site. *Fisheries Oceanography*, 22: 371–387.
- Plourde, S., Joly, P., Runge, J. A., Zakardjian, B., and Dodson, J. J. 2001. Life cycle of *Calanus finmarchicus* in the lower St. Lawrence Estuary: the imprint of circulation and late timing of the spring phytoplankton bloom. *Canadian Journal of Fisheries and Aquatic Sciences*, 58: 647–658.
- Preziosi, B. M., and Runge, J. A. 2014. The effect of warm temperatures on hatching success of the marine planktonic copepod, *Calanus finmarchicus*. *Journal of Plankton Research*, 36: 1381–1384.
- Reygondeau, G., and Beaugrand, G. 2011. Future climate-driven shifts in distribution of *Calanus finmarchicus*. *Global Change Biology*, 17: 756–766.
- Runge, J. A., Ji, R., Thompson, C. R. S., Record, N. R., Chen, C., Vandemark, D. C., Salisbury, J. E. *et al.* 2015. Persistence of *Calanus finmarchicus* in the western Gulf of Maine during recent extreme warming. *Journal of Plankton Research*, 37: 221–232.
- Runge, J. A., Jones, R. J., Record, N. R., and Pershing, A. J. 2012. Summer distribution of the planktonic copepod, *Calanus finmarchicus*, along the coast of the Gulf of Maine. Report for the State of Maine’s Department of Marine Resources.
- Saba, V. S., Griffies, S. M., Anderson, W. G., Winton, M., Alexander, M. A., Delworth, T. L., Hare, J. A., Harrison, M. J., Rosati, A., Vecchi, G. A., and Zhang, R. 2016. Enhanced warming of the Northwest Atlantic Ocean under climate change. *Journal of Geophysical Research-Oceans*, 121: 118–132.
- Sameoto, D. D., and Herman, A. W. 1990. Life cycle and distribution of *Calanus finmarchicus* in deep basins on the Nova Scotia shelf and seasonal changes in *Calanus spp.* *Marine Ecology Progress Series*, 66: 225–237.
- Shearman, R. K., and Lentz, S. J. 2010. Long-Term Sea Surface Temperature Variability along the U.S. East Coast. *Journal of Physical Oceanography*, 40: 1004–1017.
- Sun, Y. 2014. Long-and-short-term oceanic responses to atmospheric forcing over the Gulf of Maine and New England Shelf. Ph.D. dissertation, School of Marine Science, University of Massachusetts, Dartmouth. 181 pp.

- Sun, Y., Chen, C., Beardsley, R. C., Ullman, D., Butman, B., and Lin, H. 2016. Surface circulation in Block Island Sound and adjacent coastal and shelf regions: a FVCOM-CODAR comparison. *Progress in Oceanography*, 143: 26–45.
- Tian, R., Chen, C., and Qi, J. 2014. Model study of nutrient and phytoplankton dynamics in the Gulf of Maine: patterns and drivers for seasonal and interannual variability. *ICES Journal of Marine Science*, 72: 388–402.
- True, A. C., Webster, D. R., Weissburg, M. J., Yen, J., and Genin, A. 2015. Patchiness and depth-keeping of copepods in response to simulated frontal flows. *Marine Ecology Progress Series*, 539: 65–76.
- Villarino, E., Chust, G., Licandro, P., Butenschön, M., Ibaibarriaga, L., Larrañaga, A., and Irigoien, X. 2015. Modelling the future biogeography of North Atlantic zooplankton communities in response to climate change. *Marine Ecology Progress Series*, 531: 121–142.
- Woodson, C. B., Webster, D. R., Weissburg, M. J., and Yen, J. 2005. Response of copepods to physical gradients associated with structure in the ocean. *Limnology and Oceanography*, 50: 1552–1564.
- Woodson, C. B., Webster, D. R., Weissburg, M. J., and Yen, J. 2007. The prevalence and implications of copepod behavioral responses to oceanographic gradients and biological patchiness. *Integrative and Comparative Biology*, 47: 831–846.
- Xue, P., Chen, C., Qi, J., Beardsley, R. C., Tian, R., Zhao, L., and Lin, H. 2014. Mechanism studies of seasonal variability of dissolved oxygen in Mass Bay: a multi-scale FVCOM/UG-RCA application. *Journal of Marine Systems*, 131: 102–119.
- Zakardjian, B. A., Runge, J. A., Plourde, S., and Gratton, Y. 1999. A biophysical model of the interaction between vertical migration of crustacean zooplankton and circulation in the Lower St. Lawrence Estuary. *Canadian Journal of Fisheries and Aquatic Sciences*, 56: 2420–2432.

Handling editor: Brock Woodson